

Supporting Information

Unusual Molecular Mechanism behind the Thermal Response of Polypeptoids in Aqueous Solutions

*Jianbo Ma, Sunting Xuan, Abby Guerin, Tianyi Yu, Donghui Zhang, Daniel G. Kuroda**

Department of Chemistry, Louisiana State University, Baton Rouge, LA 70803, USA

*E-mail: dkuroda@lsu.edu

Synthesis

General considerations. All the chemicals and solvents used in this work were all purchased from Sigma Aldrich. All anhydrous solvents used were purified by passing through alumina columns under argon. *N*-ethyl *N*-carboxyanhydride (Et-NCA) and *N*-butyl *N*-carboxyanhydride (Bu-NCA) were synthesized by following a reported procedure.¹ All polymerization reactions were conducted under a nitrogen atmosphere.¹

¹H NMR spectra were recorded on a Bruker AV-400 nanobay spectrometer and the chemical shifts were given in parts per million (ppm) in deuterated solvents (CDCl₃). Matrix-assisted laser desorption ionization-time of flight (MALDI-TOF) mass spectra were collected on a Bruker ProFLEX III MALDI-TOF mass spectrometer in the reflector mode with *a*-cyano-4-hydroxycinnamic acid (CHCA) as the matrix. SEC analyses were performed using an Agilent 1200 system (Agilent 1200 series degasser, isocratic pump, auto sampler and column heater)

equipped with three Phenomenex 5 μm , 300 \times 7.8 mm columns, a Wyatt OptilabrEX differential refractive index (DRI) detector with a 690 nm light source, and a Wyatt DAWN EOS multiangle light scattering (MALS) detector (GaAs 30mW laser at $\lambda=690$ nm). DMF with 0.1M LiBr was used as the eluent at a flow rate of 0.5mL min^{-1} . The column and detector temperature was 25 $^{\circ}\text{C}$. The standard used was twenty three pauci-disperse polystyrene standards (590g $\cdot\text{mol}^{-1}$ -1472 kg $\cdot\text{mol}^{-1}$ MW, Polymer Laboratories, Inc.). All data analysis was performed using Wyatt Astra V 5.3 software.

Monomer Synthesis. Et-NCA and Bu-NCA were synthesized by reported literature procedures.¹⁻²

Synthesis of *c*-NHC-P(NEG-r-NBG). The polymer was synthesized by a reported procedure.¹ Briefly, inside the glovebox, stock solutions of Et-NCA (1.50 mL, 0.4 M, 0.60mmol) and Bu-NCA (0.38 mL, 0.4 M, 0.15mmol) in toluene were mixed into a small vial. A volume of 2,6-diisopropylphenylimidazol-2-ylidene (NHC)/toluene stock solution (75.8 μL , 7.5 μmol , 99.0mM) was added to the above mixture and heated at 50 $^{\circ}\text{C}$ for 24 h. Aliquots were taken and analyzed by FT-IR to check conversion. The polymer was precipitated out by adding excess hexane. The polymer was collected by filtration and dried under vacuum to obtain the final product as a pale yellow solid (53mg, 85% yield). ^1H NMR (δ in CDCl_3 , ppm): 1.14-1.15 (m, CH_3CH_2 -, NEG), 0.92-0.94 (m, CH_3CH_2 -, NBG), 1.25-1.51 (m, $\text{CH}_3\text{CH}_2\text{CH}_2$ -), 3.42-3.47 (m, $\text{CH}_3\text{CH}_2\text{N}$ -, $\text{CH}_3\text{CH}_2\text{CH}_2\text{CH}_2\text{N}$ -), 4.0-4.2 (m, $-\text{COCH}_2$ -), 7.39 (d, $-\text{CCHCHCHC}$ -, NHC end group), 7.66 (t, $-\text{CCHCHCHC}$ -, NHC end group), 7.93 (s, $-\text{NCHCHN}$ -, NHC end group).

Synthesis of *l*-NHC-P(NEG-r-NBG). The polymer was synthesized by a reported procedure.¹ *c*-NHC-P(NEG₈₀-r-NBG₂₂) (30mg, 3.1 μmol) was dissolved in anhydrous toluene (1 mL) followed by the addition of acyl chloride/toluene solution (38 μL , 34 μmol , 0.9 M). The reaction mixture

was stirred at room temperature for 20 min and excess hexane was added to precipitate the polymer. The polymer was collected by filtration and dried under vacuum to obtain the final product as a white solid (26.7 mg, 89% yield). ^1H NMR (δ in CDCl_3 , ppm): 1.14-1.16 (m, CH_3CH_2- , NEG), 0.88-0.94 (m, CH_3CH_2- , NBG), 1.23-1.52 (m, $\text{CH}_3\text{CH}_2\text{CH}_2-$), 3.48 (m, $\text{CH}_3\text{CH}_2\text{N}-$, $\text{CH}_3\text{CH}_2\text{CH}_2\text{CH}_2\text{N}-$), 4.1-4.2 (m, $-\text{COCH}_2-$), 7.41 (d, $-\text{CCHCHCHC}-$, NHC end group), 7.62 (t, $-\text{CCHCHCHC}-$, NHC end group), 8.10 (s, $-\text{NCHCHN}-$, NHC end group).

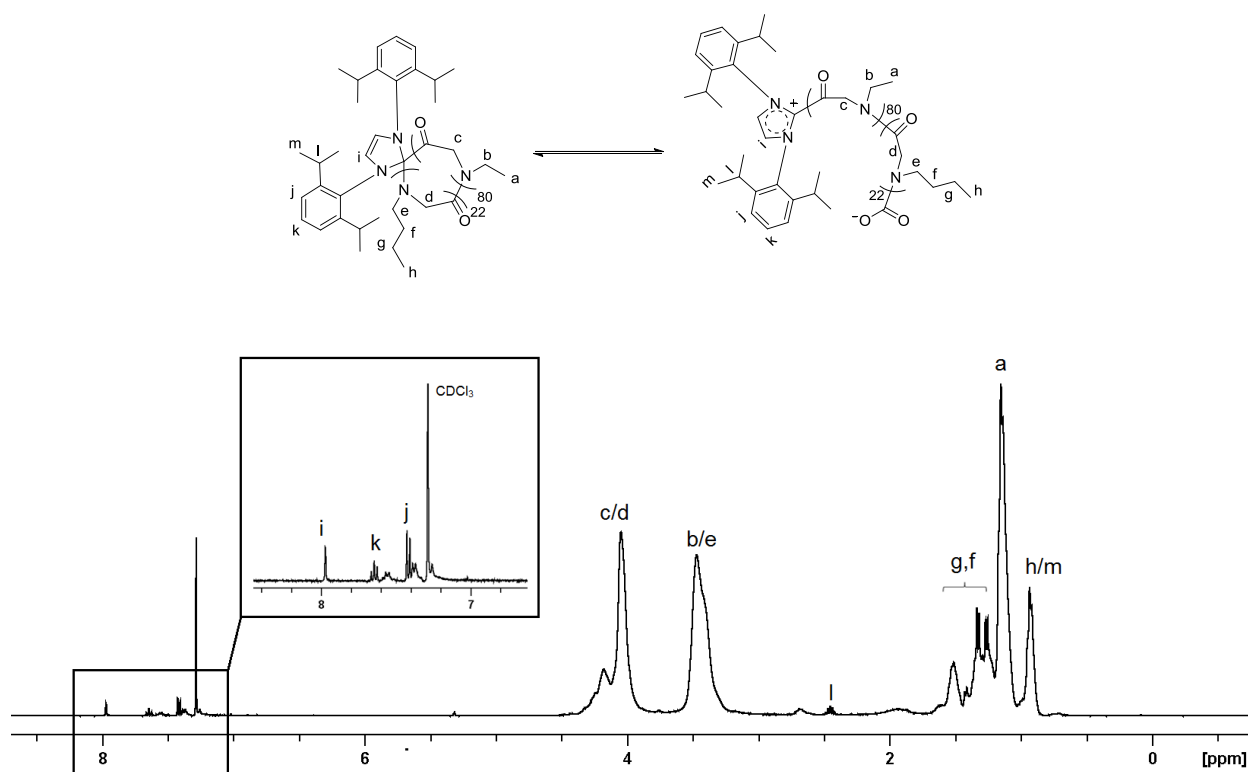


Figure S1. ^1H NMR spectrum of c-NHC-P(NEG₈₀-r-NBG₂₂) in CDCl_3 .

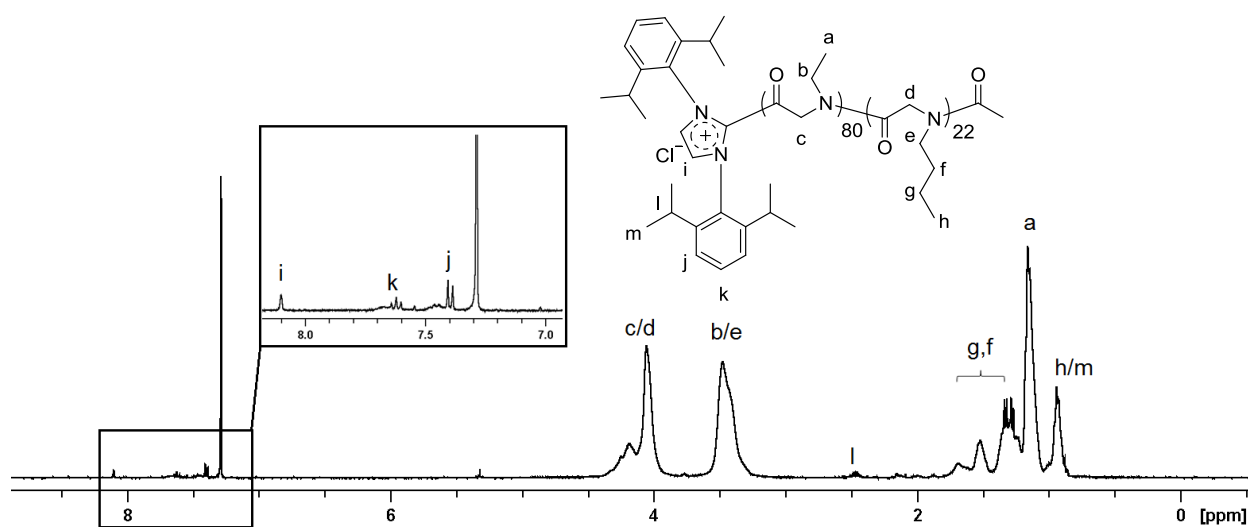


Figure S2. ^1H NMR spectrum of *l*-NHC-P(NEG₈₀-r-NBG₂₂) in CDCl_3 .

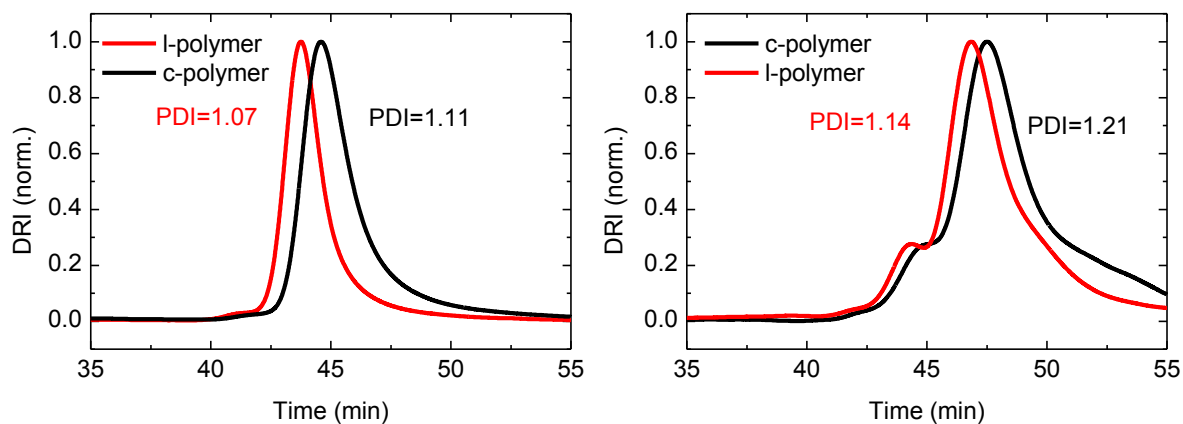


Figure S3. SEC-DRI chromatograms of the cyclic polymer *c*-NHC-P(NEG₈₀-r-NBG₂₂) (red line) and the corresponding linear analog *l*-NHC-P(NEG₈₀-r-NBG₂₂) (black line) obtained by treating the cyclic polymer precursor with acyl chloride in DMF/LiBr (0.1M) at rt. chromatograms obtained by direct injection of the polymerization mixture into the SEC column versus that of polymer isolated by precipitation and drying. The high molecular weight shoulders in the SEC chromatograms of the dried polymer samples were attributed to the polymer aggregates due to the incomplete dissolution of the polymer in the SEC solvent (0.1 M LiBr/DMF, rt).^{1,6}

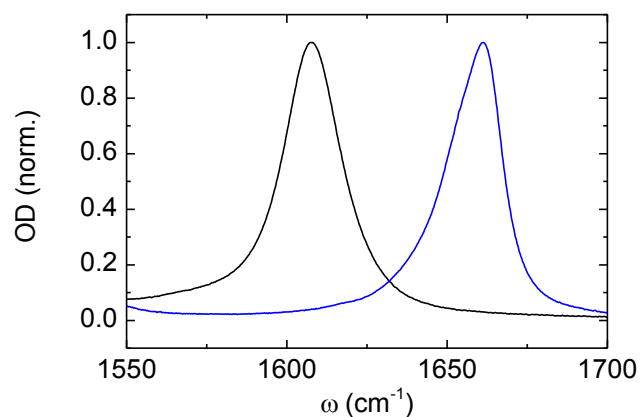


Figure S4. IR spectra of DMA in D₂O (black) and THF (blue) at the amide I range.

Two Dimensional IR spectroscopy (2D IR)

In short, the 2D IR spectra shows two peaks Figure S5 and S6 show the 2D IR spectra of the two aqueous solutions at two waiting times: 0.25ps and 1ps. At any waiting time, two peaks are observed in the 2D IR spectra. While the red band (right) correspond to transitions involving the ground state and the first excited vibrational state, the blue band (left) is assigned to transitions comprising the first and second vibrational states.³ The 2D IR spectra has been mainly used to examine the dynamics of the molecular environment of a molecule in solution.³ In the case of these polymers the large inhomogeneity of the polymer sample and/or the environment of the different amide I units does not allow us to retrieve such information. However, the second dimension of the spectra and the vibrational lifetime of the components of the amide I, which is also dependent on the environment, allows us to assign the number of components in the spectra.⁴ The analysis of the spectra versus waiting time shows that the spectra are composed of two at 1635 cm⁻¹ and 1655 cm⁻¹. Although the intensity of the 1635 cm⁻¹ peak is not so obvious in 2D IR spectra compared to the FTIR spectra, as the waiting time increases to 1.0 picosecond, this low frequency peak is barely observable which indicated that its vibrational lifetime is shorter than that of the high frequency peak (1655 cm⁻¹). This observation is confirmed by

computing the difference in intensity of the positive peak diagonal at different frequencies as a function of the waiting time (Figure 4 of the manuscript). From these results, it is concluded that the low frequency peak (located at 1635 cm^{-1}) decays faster than the frequency high one (located at 1655 cm^{-1}). The observed difference in vibrational lifetime are consistent with a difference in the solvation environment of the polymer units.⁵

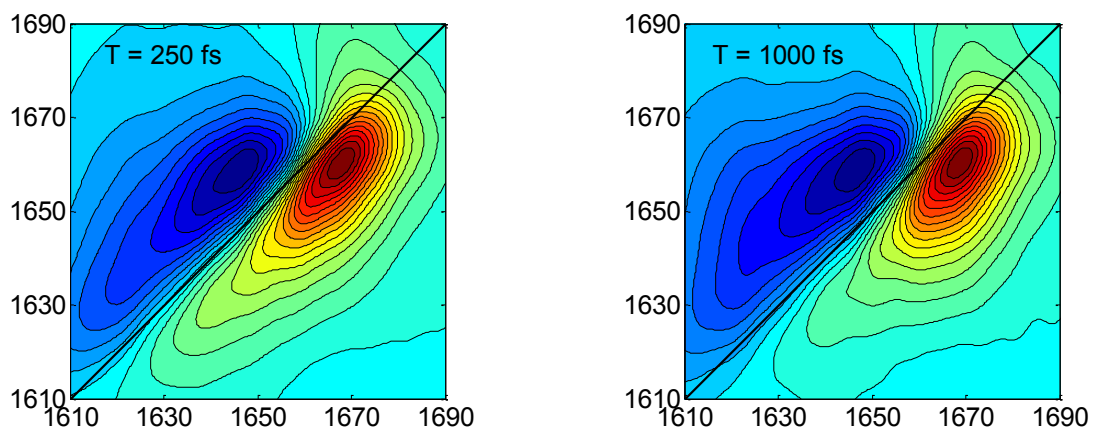


Figure S5. The 2D IR spectra of the linear copolymer at two different waiting times

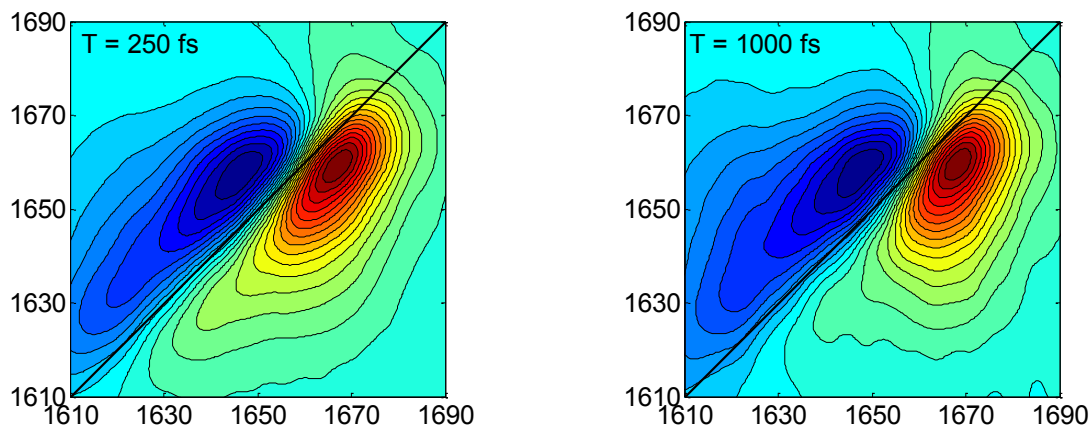


Figure S6. The 2D IR spectra of the cyclic copolymer at two different waiting times.

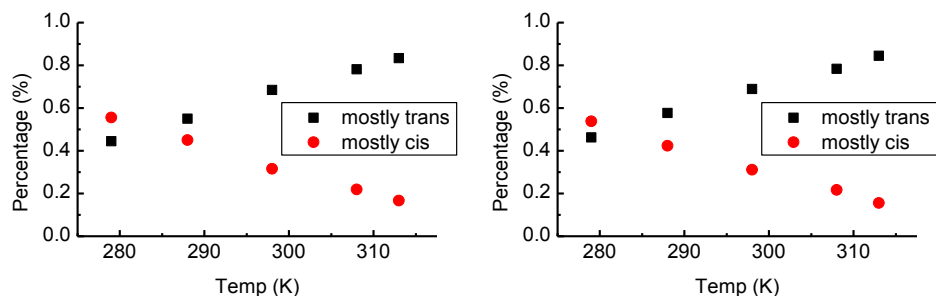


Figure S7. Ratio of NMR areas for the mostly *cis* and mostly *trans* alpha-hydrogens of the polypeptoid as function of temperature. The linear and cyclic polypeptoid samples are presented in the left and right plots, respectively.

Determination of the enthalpy of phase transition

The enthalpy of the phase transition was determined from the fraction of backbone amide I units having *cis* amide I (PPL) conformation. Note that this methodology has been previously used by Schonhoff et. al. to determine the phase transition of PNIPAM via NMR.⁷ The equilibrium constant expressed as the ratio of the areas of the PPL I conformation over the random polymer [RP].

$$K = \frac{[PPLI]_{eq}}{[RP]_{eq}}$$

The temperature dependence of the equilibrium constant expressed as:⁸

$$\ln \frac{A_{PPLI}}{A_{RP}} = -\frac{\Delta H^0}{RT} + \frac{\Delta S^0}{R} - \ln\left(\frac{\epsilon_{RP}}{\epsilon_{PPLI}}\right)$$

where A_{PPLI} and A_{RP} are the areas determined from the fitting the FTIR spectra. Thus, the enthalpy of the initial and final states (i.e., before and after phase transition) can be determined from the plots of $\ln([A_{PPLI}/A_{RP}])$ vs $1/T$. Moreover, the enthalpy of the phase transition can be calculated from:

$$\Delta H_{PT} = \Delta H_{final} - \Delta H_{initial}$$

where ΔH_{final} and $\Delta H_{initial}$ are the enthalpies derived from the van't Hoff plots of the equilibrium constant before and after the phase transition (Figure S8).

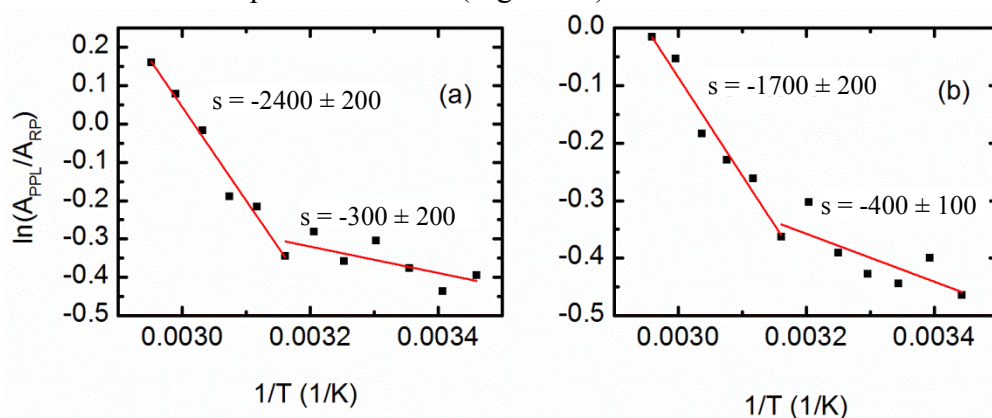


Figure S8. Van't Hoff plots for the equilibrium constants of the conformational change in both the linear (a) and the cyclic (b) polymers.

Table S1. Fitting results for linear polymer. (y0: offset; xc: central wavenumber; A: area; wG: Gaussian FWHM; wL: Lorentzian FWHM)

Temp (°C)	16.00	20.53	25.11	29.74	34.39	38.95	43.43	47.89	52.35	56.82	61.45	65.83
y0	0.04	0.04	0.05	0.06	0.08	0.10	0.12	0.13	0.13	0.14	0.16	0.16
xc1 (cm ⁻¹)	1635.16	1635.63	1635.53	1636.29	1637.16	1637.29	1638.18	1637.75	1638.22	1636.64	1636.09	1635.77
A1	1.26	1.20	1.12	1.14	1.20	1.17	1.21	1.25	1.33	1.29	1.20	1.16
wG1	16.09	16.84	16.25	16.32	16.84	16.80	17.21	15.73	15.46	12.56	11.44	11.00
wL1	1.01	0.00	0.00	0.00	0.00	0.00	0.00	2.32	3.48	6.41	6.85	7.06
xc2 (cm ⁻¹)	1656.06	1656.12	1656.08	1656.51	1656.94	1657.06	1657.48	1657.48	1657.96	1657.71	1657.82	1657.99
A2	0.79	0.77	0.79	0.84	0.82	0.89	0.87	0.99	1.07	1.22	1.27	1.33
wG2	11.39	11.39	11.41	10.86	10.55	10.23	10.11	10.28	10.20	11.64	12.97	13.81
wL2	0.00	0.06	0.01	1.11	1.56	2.46	2.68	3.04	3.75	2.43	0.87	0.00
xc3 (cm ⁻¹)	1549.42	1547.55	1542.38	1541.27	1536.59	1530.85	1525.43	1520.19	1517.28	1511.87	1502.98	1498.50
A3	256.56	263.94	268.76	270.81	274.27	274.59	273.64	279.44	301.66	315.96	326.96	349.47
wG3	0.40	0.02	30.49	24.76	35.86	49.54	61.63	67.31	59.91	64.05	78.64	78.82
wL3	148.16	150.60	147.63	149.18	146.44	139.91	132.14	129.12	138.46	138.32	129.57	132.94

Table S2. Fitting results for cyclic polymer.

Temp (°C)	17.41	21.72	26.06	30.37	34.66	39.08	43.38	47.76	52.03	56.25	60.74	64.96
y0	0.04	0.04	0.05	0.06	0.06	0.09	0.09	0.14	0.15	0.14	0.18	0.17
xc1 (cm ⁻¹)	1635.20	1635.48	1635.96	1636.31	1635.71	1636.66	1637.81	1637.53	1638.00	1638.21	1637.08	1636.64
A1	1.58	1.51	1.57	1.57	1.66	1.52	1.65	1.54	1.66	1.79	1.73	1.77
wG1	16.55	16.29	16.60	16.73	15.25	16.58	17.38	16.85	16.34	15.35	13.07	11.59
wL1	0.08	0.00	0.01	0.00	2.47	0.00	0.00	0.00	1.55	3.55	5.81	7.55
xc2 (cm ⁻¹)	1656.19	1656.24	1656.55	1656.70	1656.50	1656.97	1657.46	1657.51	1657.86	1658.31	1658.19	1658.40
A2	0.99	1.00	0.99	1.02	1.07	1.11	1.11	1.19	1.29	1.41	1.61	1.70
wG2	11.37	11.32	11.35	10.96	11.55	10.75	9.87	10.30	9.90	9.82	11.14	12.19
wL2	0.00	0.00	0.00	0.69	0.00	1.45	2.86	2.50	3.60	4.34	3.39	2.40
xc3 (cm ⁻¹)	1550.87	1550.13	1544.82	1542.63	1535.30	1531.90	1530.31	1518.61	1515.97	1514.59	1503.09	1500.28
A3	250.19	252.35	268.75	267.99	286.66	268.27	285.39	253.33	272.91	298.56	294.21	326.14
wG3	0.03	0.01	6.86	19.30	29.70	50.96	40.76	83.70	77.27	64.75	88.11	80.20
wL3	146.83	147.48	152.68	150.33	153.55	138.15	147.00	109.97	119.73	133.86	113.62	126.11

Table S3. FWHM of the amide I band as function of temperature (error in Temperature $\pm 0.1^\circ\text{C}$ and in wavelength $\pm 0.1 \text{ cm}^{-1}$)

Sample	Cyclic polymer											
T/°C	17.4	21.7	26.1	30.4	34.7	39.1	43.4	47.8	52.0	56.3	60.7	65.0
FWHM / cm ⁻¹	46.5	46.2	46.1	45.8	45.9	45.6	45.3	45.2	45.3	45.3	45.6	45.9
Sample	Linear polymer											
T/°C	16.0	20.5	25.1	29.7	34.4	39.0	43.4	47.9	52.4	56.8	61.4	65.8
FWHM/ cm ⁻¹	47.5	47.3	46.7	46.5	46.6	46.5	46.1	46.0	45.8	45.9	46.0	46.3

References

1. Lahasky, S. H.; Hu, X. K.; Zhang, D. H., Thermoresponsive Poly(alpha-peptoid)s: Tuning the Cloud Point Temperatures by Composition and Architecture. *Acs Macro Lett* **2012**, *1* (5), 580-584.
2. Guo, L.; Zhang, D. H., Cyclic Poly(alpha-peptoid)s and Their Block Copolymers from N-Heterocyclic Carbene-Mediated Ring-Opening Polymerizations of N-Substituted N-Carboxyanhydrides. *J Am Chem Soc* **2009**, *131* (50), 18072.
3. Hamm, P.; Zanni, M. T., *Concepts and methods of 2d infrared spectroscopy*. Cambridge University Pres: Cambridge ; New York, 2011; p ix, 286 p.
4. Kuroda, D. G.; Hochstrasser, R. M., Dynamic structures of aqueous oxalate and the effects of counterions seen by 2D IR. *Phys Chem Chem Phys* **2012**, *14* (18), 6219-6224.
5. Middleton, C. T.; Buchanan, L. E.; Dunkelberger, E. B.; Zanni, M. T., Utilizing Lifetimes to Suppress Random Coil Features in 2D IR Spectra of Peptides. *J Phys Chem Lett* **2011**, *2* (18), 2357-2361.
6. Lahasky, S. H.; Serem, W. K.; Guo, L.; Garno, J. C.; Zhang, D. Synthesis and Characterization of Cyclic Brush-Like Polymers by N-Heterocyclic Carbene-Mediated Zwitterionic Polymerization of N-Propargyl N-Carboxyanhydride and the Grafting-to Approach. *Macromolecules* **2011**, *44*, 9063-9074.
7. Spěváček, J.; NMR investigations of phase transition in aqueous polymer solutions and gels. *Curr Opin Colloid Interface Sci* **2009**, *14*, 184-191.
8. Guerin A.C.; Riley K.; Rupnik K.; Kuroda D.G., "Determining the Energetics of the Hydrogen Bond through FTIR: A Hands-On Physical Chemistry Lab Experiment", *J Chem Ed* **2016**, *93*, 1124-1129.